



**HAL**  
open science

## Raman investigation of air-stable silicene nanosheets on an inert graphite surface

Paola Castrucci, Filippo Fabbri, Tiziano Delise, Manuela Scarselli, Matteo Salvato, Sara Pascale, Roberto Francini, Isabelle Berbezier, Christoph Lechner, Fatme Jardali, et al.

### ► To cite this version:

Paola Castrucci, Filippo Fabbri, Tiziano Delise, Manuela Scarselli, Matteo Salvato, et al.. Raman investigation of air-stable silicene nanosheets on an inert graphite surface. Nano Research, 2018, 10.1007/s12274-018-2097-6 . hal-02395212

**HAL Id: hal-02395212**

**<https://hal.science/hal-02395212>**

Submitted on 5 Dec 2019

**HAL** is a multi-disciplinary open access archive for the deposit and dissemination of scientific research documents, whether they are published or not. The documents may come from teaching and research institutions in France or abroad, or from public or private research centers.

L'archive ouverte pluridisciplinaire **HAL**, est destinée au dépôt et à la diffusion de documents scientifiques de niveau recherche, publiés ou non, émanant des établissements d'enseignement et de recherche français ou étrangers, des laboratoires publics ou privés.

## **Raman investigation of air-stable silicene nanosheets on an inert graphite surface**

Paola Castrucci, Filippo Fabbri, Tiziano Delise, Manuela Scarselli, Matteo Salvato, Sara Pascale, Roberto Francini, Isabelle Berbezier, Christoph Lechner, Fatme Jardali, et al.

► **To cite this version:**

Paola Castrucci, Filippo Fabbri, Tiziano Delise, Manuela Scarselli, Matteo Salvato, et al.. Raman investigation of air-stable silicene nanosheets on an inert graphite surface. Nano Research, Springer, 2018. hal-02395212

**HAL Id: hal-02395212**

**<https://hal.archives-ouvertes.fr/hal-02395212>**

Submitted on 5 Dec 2019

**HAL** is a multi-disciplinary open access archive for the deposit and dissemination of scientific research documents, whether they are published or not. The documents may come from teaching and research institutions in France or abroad, or from public or private research centers.

L'archive ouverte pluridisciplinaire **HAL**, est destinée au dépôt et à la diffusion de documents scientifiques de niveau recherche, publiés ou non, émanant des établissements d'enseignement et de recherche français ou étrangers, des laboratoires publics ou privés.

# Nano Research

## Raman investigation of air-stable silicene nanosheets on an inert graphite surface --Manuscript Draft--

<b>Manuscript Number:</b>		
<b>Full Title:</b>	Raman investigation of air-stable silicene nanosheets on an inert graphite surface	
<b>Article Type:</b>	Regular Article	
<b>Corresponding Author:</b>	Paola Castrucci Università degli Studi di Roma Tor Vergata Dipartimento di Fisica ITALY	
<b>Corresponding Author Secondary Information:</b>		
<b>Corresponding Author's Institution:</b>	Università degli Studi di Roma Tor Vergata Dipartimento di Fisica	
<b>Corresponding Author's Secondary Institution:</b>		
<b>First Author:</b>	Paola Castrucci	
<b>First Author Secondary Information:</b>		
<b>Order of Authors:</b>	Paola Castrucci	
	Filippo Fabbri	
	Tiziano Delise	
	Manuela Scarselli	
	Matteo Salvato	
	Sara Pascale	
	Roberto Francini	
	Isabelle Berbezier	
	Christoph Lechner	
	Fatme Jardali	
	Holger Vach	
	Maurizio De Crescenzi	
<b>Order of Authors Secondary Information:</b>		
<b>Funding Information:</b>	Università degli Studi di Roma Tor Vergata (IT)	Prof. Paola Castrucci
	Università degli Studi di Roma Tor Vergata	Dr. Matteo Salvato Prof. Maurizio De Crescenzi
	European Community-RISE (GA644076)	Dr. Manuela Scarselli
	European community: RISE (GA644076)	Dr. Matteo Salvato
	European Community RISE (GA644076)	Prof. Paola Castrucci Prof. Maurizio De Crescenzi
	HPC centers (i2016-090642)	Dr. Christoph Lechner
	HPC centers (i2016-090642)	Dr. Fatme Jardali Prof. Holger Vach
	Hariri Foundation for Sustainable Human Development	Dr. Fatme Jardali

<b>Abstract:</b>	<p>The fascinating properties of two dimensional (2D) crystals have gained increasing interest for many applications. In this regard, the synthesis of a 2D silicon structure, namely silicene, is attracting great interest for possible development of next generation micro- and nano-electronic devices. The main difficulty in working with silicene remains its strong tendency to oxidation when exposed to air as a consequence of its relatively highly buckled structure. In this work, we univocally identify the Raman mode of air-stable low-buckled silicene nanosheets synthesized on highly oriented pyrolytic graphite (HOPG) located at 542.5 cm<sup>-1</sup>. The main focus of this work is Raman spectroscopy and mapping analyses in combination with ab initio calculations. Scanning tunneling microscopy images reveal the presence of a patchwork of Si three-dimensional (3D) islands and contiguous Si areas presenting a honeycomb atomic arrangement, rotated by 30° with respect to the HOPG substrate underneath, with a lattice parameter of 0.41 ± 0.02 nm and a buckling of the Si atoms of 0.05 nm. Raman analysis supports the co-existence of 3D silicon clusters and 2D silicene structures. The Raman shift of low-buckled silicene on an inert substrate has not been reported so far and it is completely different from both; the one calculated for free-standing silicene and the experimental ones measured for silicene grown on Ag(111) surfaces. Our experimental results are perfectly reproduced by our ab initio calculations of silicene nanosheets. This leads us to the conclusion that the precise value of the observed Raman shift crucially depends on the strain induced between the silicene nanosheets and the graphite substrate.</p>
<b>Suggested Reviewers:</b>	<p>Serge Lefrant Serge.Lefrant@cnsr-imn.fr International reknown expert of Raman</p> <hr/> <p>Peter Voorhees p-voorhees@northwestern.edu expert of growth of nanowires and nanomaterials</p> <hr/> <p>Kastern Horn horn@fhi-berlin.mpg.de Internationally reputed expert on the growth and characterization of graphene and other 2D materials</p> <hr/> <p>Guy Le Lay guy.lelay@univ-amu.fr Outstanding researcher on growth of silicon on several substrate and in particular he developed the method to grow silicene on silver</p> <hr/> <p>Emilio Scalise scalise@mpie.de Theoretician who calculated Raman modes of silicene</p> <hr/> <p>Bene Poelsema b.poelsema@utwente.nl Outstanding researcher on 2D material growth</p>

1  
2  
3  
4  
5  
6  
7  
8  
9  
10  
11  
12  
13  
14  
15  
16  
17  
18  
19  
20  
21  
22  
23  
24  
25  
26  
27  
28  
29  
30  
31  
32  
33  
34  
35  
36  
37  
38  
39  
40  
41  
42  
43  
44  
45  
46  
47  
48  
49  
50  
51  
52  
53  
54  
55  
56  
57  
58  
59  
60  
61  
62  
63  
64  
65

# Raman investigation of air-stable silicene nanosheets on an inert graphite surface

*Paola Castrucci*<sup>1,\*</sup>, *Filippo Fabbri*<sup>2,\*</sup>, *Tiziano Delise*<sup>1</sup>, *Manuela Scarselli*<sup>1</sup>, *Matteo Salvato*<sup>1</sup>,  
*Sara Pascale*<sup>3</sup>, *Roberto Francini*<sup>4</sup>, *Isabelle Berbezier*<sup>5</sup>, *Christoph Lechner*<sup>6</sup>, *Fatme Jardali*<sup>7</sup>,  
*Holger Vach*<sup>7,\*</sup>, and *Maurizio De Crescenzi*<sup>1</sup>

<sup>1</sup> Dipartimento di Fisica, Università di Roma “Tor Vergata”, 00133 Roma, Italy

<sup>2</sup> Center for Nanotechnology Innovation c/o NEST, Istituto Italiano di Tecnologia, 56127 Pisa,  
Italy

<sup>3</sup> Consorzio di Ricerca Hypatia, c/o Italian Space Agency, 00133 Roma, Italy

<sup>4</sup> Dipartimento di Ingegneria Industriale, Università di Roma “Tor Vergata”, 00133 Roma, Italy

<sup>5</sup> CNRS, Aix-Marseille Université, IM2NP, UMR 7334, 13397 Marseille, France

<sup>6</sup> EDF R&D, Department Materials and Mechanics of Components (MMC), Moret-sur-Loing,  
France

<sup>7</sup> CNRS-LPICM, Ecole Polytechnique, Université Paris-Saclay, 91128 Palaiseau, France

1  
2  
3  
4  
5  
6  
7 \* Corresponding authors: castrucci@roma2.infn.it; filippo.fabbri@iit.it,  
8  
9 holger.vach@polytechnique.edu  
10

## 11 12 13 **ABSTRACT** 14

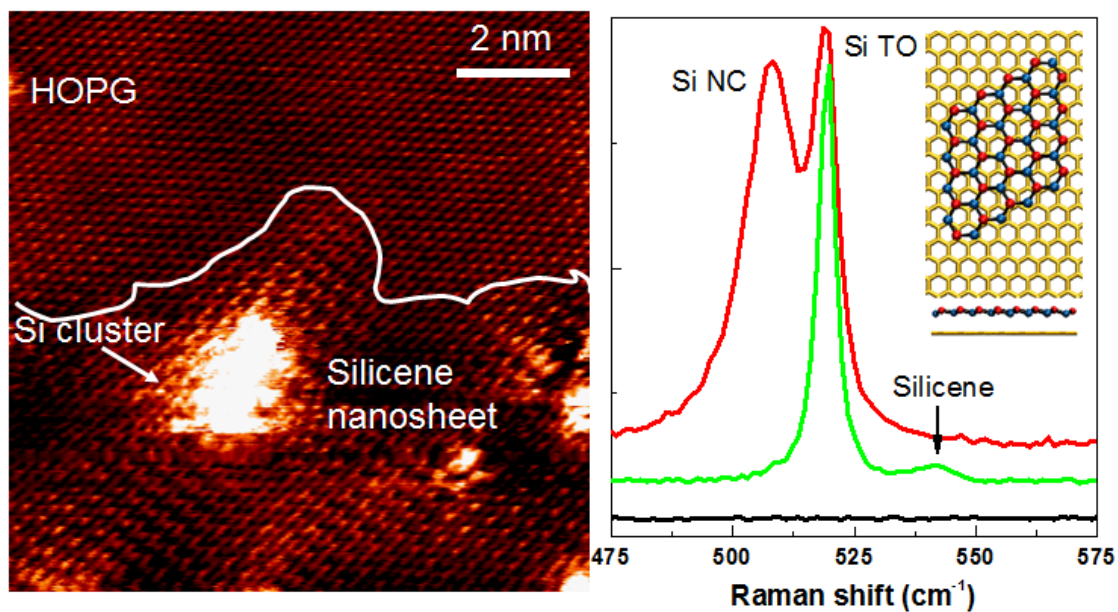
15  
16  
17 The fascinating properties of two dimensional (2D) crystals have gained increasing interest for  
18 many applications. In this regard, the synthesis of a 2D silicon structure, namely silicene, is  
19 attracting great interest for possible development of next generation micro- and nano-electronic  
20 devices. The main difficulty in working with silicene remains its strong tendency to oxidation  
21 when exposed to air as a consequence of its relatively highly buckled structure. In this work, we  
22 univocally identify the Raman mode of air-stable low-buckled silicene nanosheets synthesized on  
23 highly oriented pyrolytic graphite (HOPG) located at  $542.5 \text{ cm}^{-1}$ . The main focus of this work is  
24 Raman spectroscopy and mapping analyses in combination with *ab initio* calculations. Scanning  
25 tunneling microscopy images reveal the presence of a patchwork of Si three-dimensional (3D)  
26 islands and contiguous Si areas presenting a honeycomb atomic arrangement, rotated by  $30^\circ$  with  
27 respect to the HOPG substrate underneath, with a lattice parameter of  $0.41 \pm 0.02 \text{ nm}$  and a  
28 buckling of the Si atoms of  $0.05 \text{ nm}$ . Raman analysis supports the co-existence of 3D silicon  
29 clusters and 2D silicene structures. The Raman shift of low-buckled silicene on an inert substrate  
30 has not been reported so far and it is completely different from both; the one calculated for free-  
31 standing silicene and the experimental ones measured for silicene grown on Ag(111) surfaces. Our  
32 experimental results are perfectly reproduced by our *ab initio* calculations of silicene nanosheets.  
33  
34 This leads us to the conclusion that the precise value of the observed Raman shift crucially depends  
35 on the strain induced between the silicene nanosheets and the graphite substrate.  
36  
37  
38  
39  
40  
41  
42  
43  
44  
45  
46  
47  
48  
49  
50  
51  
52  
53  
54  
55  
56  
57  
58  
59  
60  
61  
62  
63  
64  
65

1  
2  
3  
4  
5  
6  
7  
8  
9  
10  
11  
12  
13  
14  
15  
16  
17  
18  
19  
20  
21  
22  
23  
24  
25  
26  
27  
28  
29  
30  
31  
32  
33  
34  
35  
36  
37  
38  
39  
40  
41  
42  
43  
44  
45  
46  
47  
48  
49  
50  
51  
52  
53  
54  
55  
56  
57  
58  
59  
60  
61  
62  
63  
64  
65

Keywords: 2D Materials, Silicene, Raman spectroscopy, ab initio calculations, scanning tunneling  
microscopy, scanning tunneling spectroscopy.

[Click here to view linked References](#)

## Graphical Table of Contents



We have identified the Raman mode of *air-stable* low-buckled (with  $sp^2$  configuration) silicene nanosheets synthesized on highly oriented pyrolytic graphite located at  $542.5 \text{ cm}^{-1}$ . Scanning tunneling microscopy images support the growth of low-buckled honeycomb structure. Our experimental results are perfectly reproduced by our *ab initio* calculations of silicene nanosheets.

1  
2  
3  
4 1. Introduction  
5

6 Graphene, one of the allotropes of carbon, is an atomically flat single sheet which exhibits a  
7 honeycomb structure with  $sp^2$  hybridization of the carbon atoms. [1] Individual graphene layers  
8 were first isolated by cleaving graphite using “adhesive tape.” [1,2] This material demonstrates  
9 superior electrical and mechanical properties, in fact displaying a room temperature quantum Hall  
10 effect, [3,4] and more importantly, it is the strongest material reported to date. [4] Graphene is a  
11 semimetal with its conduction band and valence band being degenerate at the K point in the  
12 Brillouin zone and has an extremely high room temperature carrier mobility (about 2 orders of  
13 magnitude greater than that of silicon). [5]  
14  
15

16 Although belonging to the same group as carbon, Si preferentially tends to arrange in  $sp^3$   
17 configuration with its surrounding atoms. Even for an ultrathin film, silicon atoms deposited on a  
18 solid surface form three-dimensional (3D) diamond-like structures. [6-8] In spite of these generally  
19 accepted features, recent theoretical and experimental works have demonstrated the existence of a  
20 stable phase of single-layered silicon with graphene-like structure (generally called silicene) in a  
21 slightly puckered configuration. [9,10] Silicene has been attracting much attention for the  
22 promising improvements that its use can imply in silicon based nano-electronic devices. [11]  
23  
24

25 Raman spectroscopy of bulk silicon shows a main transverse optical (TO) peak located at 520  
26  $cm^{-1}$  while the free-standing (FS) silicene  $E_{2g}$  peak has been predicted to be between 549 and 575  
27  $cm^{-1}$  according to the calculation method used. [12,13] Recently, Raman spectra of silicene on Ag  
28 (111) substrates have revealed features markedly different from the previous ones which are  
29 located a) at around 514  $cm^{-1}$  for  $3 \times 3/4 \times 4$  epitaxial silicene on Ag(111); [14] b) ranging between  
30 515 and 522  $cm^{-1}$  for  $2\sqrt{3} \times 2\sqrt{3}$  epitaxial silicene [11] and c) at around 530  $cm^{-1}$  for epitaxial  
31  $\sqrt{13} \times \sqrt{13}/4 \times 4$  silicene. [15] This wide range of results has been associated to differences in: surface  
32  
33  
34  
35  
36  
37  
38  
39  
40  
41  
42  
43  
44  
45  
46  
47  
48  
49  
50  
51  
52  
53  
54  
55  
56  
57  
58  
59  
60  
61  
62  
63  
64  
65

1  
2  
3  
4 reconstructions, the amount of silicene buckling and/or charge doping effects. Indeed, theoretical  
5  
6 calculations support the observed red-shifting of the silicene  $E_{2g}$  mode by increasing the buckling.  
7  
8 [16] Recently, we have reported evidence that patches of silicene can grow on inert substrates such  
9  
10 as highly oriented pyrolytic graphite (HOPG). [17] The nanosheets of silicene have often been  
11  
12 detected very close to small nanosized (3D) Si clusters leaving large parts of the HOPG surface  
13  
14 free of additional nanostructures. This surface inhomogeneity has also been reported for the growth  
15  
16 of silicene nanosheets on  $MoS_2$ . [18]  
17  
18  
19  
20

21 In this work, we univocally identify the Raman mode of air-stable low-buckled silicene  
22  
23 nanosheets, grown on a HOPG substrate. We carefully studied the vibrational properties of the  
24  
25 silicon/HOPG surface by acquiring Raman maps on the micrometric scale, demonstrating the  
26  
27 coexistence of 3D silicon structures and low-buckled silicene nanosheets. We have observed  
28  
29 specific features that can be assigned to the silicene  $E_{2g}$  vibrational mode, silicon nanoclusters, and  
30  
31 the  $E_{2g}$  mode of defect-free and unperturbed HOPG (namely, the G-band). We have found the first  
32  
33 peak to be located around  $542.5 \pm 0.5 \text{ cm}^{-1}$ . We interpret this silicene  $E_{2g}$  value as being due to the  
34  
35 low buckling (about 0.05 nm) of silicon atoms in the honeycomb arrangement of silicene grown  
36  
37 on a HOPG substrate, observed by scanning tunneling microscopy (STM). Until now, this value  
38  
39 is markedly different from all the values reported in the literature for any other silicon  
40  
41 configuration and for silicene on  $Ag(111)$ . [11,14,15]  
42  
43  
44  
45  
46  
47  
48  
49

## 50 2. Experimental

51  
52 A HOPG (from GE Advanced Ceramics, USA, 12 mm  $\times$  12 mm  $\times$  1 mm) sample was used as a  
53  
54 substrate. A fresh surface of graphite was obtained by peeling the HOPG substrate with adhesive  
55  
56 tape and transferring it into a ultra-high-vacuum (UHV) chamber. High-purity silicon (Sil'tronix  
57  
58  
59  
60  
61  
62  
63  
64  
65

1  
2  
3  
4 ST,  $\rho = 1-10 \Omega \cdot \text{cm}$ , n-doped) was evaporated from a wafer located at 200 mm from the substrate.  
5  
6 The deposition was achieved under UHV conditions (base pressure low  $10^{-10}$  Torr) and at a  
7  
8 constant rate of 0.01 nm/min (0.04 ML/min) monitored by an Inficon quartz balance. Deposition  
9  
10 was carried out keeping the substrate at room temperature (RT). STM imaging was performed  
11  
12 using an Omicron-STM system with electrochemically etched tungsten tips. The STM was  
13  
14 calibrated by acquiring atomically resolved images of the bare HOPG surface. All images were  
15  
16 acquired in the constant current mode and were unfiltered apart from the rigid plane subtraction.  
17  
18 *Ex-situ* Raman spectroscopy and mapping have been performed without capping the sample. The  
19  
20 Raman analyses was carried out with a 532 nm excitation laser, a laser power density of 0.1  
21  
22  $\text{mW}/\mu\text{m}^2$  and an acquisition time of 1 s. The spectral resolution is  $2 \text{ cm}^{-1}$ . Low magnification line  
23  
24 scans were performed with a 20X objective (NA 0.40), acquiring a spectrum every 200  $\mu\text{m}$ .  
25  
26 Meanwhile, the high magnification Raman maps were obtained with a 100X objective (NA=0.85),  
27  
28 with 500 nm of lateral resolution. The Raman system is a Renishaw Invia Qtor equipped with a  
29  
30 confocal optical microscope and a high resolution Andor CCD camera. Preliminary Raman  
31  
32 characterization of the bare HOPG surface before Si deposition is reported in Fig. S1 of the  
33  
34 Electronic Supplementary Material (ESM) file. From the Voigt deconvolution, it is possible to  
35  
36 evaluate the peak position and FWHM and the associated error as  $0.5 \text{ cm}^{-1}$ .  
37  
38

39  
40  
41 *Ab initio* calculations were performed with the CRYSTAL09 software package. [19,20] The  
42  
43 Perdew–Burke–Ernzerhof functional [21] combined with Grimme's D2 dispersion correction [22]  
44  
45 ( $s_6 = 0.25$ ) was applied. Information regarding the basis set can be found in the SI. For the infinite  
46  
47 graphite-silicene interfaces, a four layer slab with AB stacking was used to model the HOPG  
48  
49 surface. Each slab consisted of 14 and 128 carbon atoms for rotation angles of 10 and 30 degrees  
50  
51 between the hexagonal patterns, respectively. For finite nano-islands, the HOPG surface was  
52  
53  
54  
55  
56  
57  
58  
59  
60  
61  
62  
63  
64  
65

1  
2  
3  
4 reduced to one graphene layer consisting of 350 and 512 carbon atoms for 10 and 30 degrees,  
5  
6 respectively. The silicene nano-islands consisted of 48 (zigzag) and 54 (armchair) Si atoms; the  
7  
8 edge atoms were saturated with hydrogen. The energy and force thresholds for the optimizations  
9  
10 and frequency calculations [23,24] were  $10^{-10}$  a.u. and  $4.5 \times 10^{-5}$  a.u. A 3x3 Monkhorst-Pack mesh  
11  
12 including the  $\Gamma$  point was used throughout except for FS silicene and the 10 degree interface where  
13  
14 a 20x20 mesh was employed. The modes which stem from the  $E_{2g}$  mode of FS silicene were  
15  
16 selected by calculating the maximum overlap (*i.e.* scalar product) between the displacement  
17  
18 vectors of the  $E_{2g}$  mode of FS silicene and those of the interface/nano-islands. A thorough  
19  
20 explanation of this approach can be found in the SI.  
21  
22  
23  
24  
25  
26

### 27 3. Results and Discussion

#### 28 3.1 Sample characterization

29  
30  
31  
32  
33 Figs. 1(a)-(c) show typical STM images, reported in a sequence with increasing magnification,  
34  
35 of 1 ML of Si deposited at RT on a HOPG surface. Si clusters are homogeneously spread on darker  
36  
37 and brighter areas of the HOPG surface, while they appear aligned decorating the straight steps of  
38  
39 substrate terraces. In Fig. 1(d) the line profile, taken along the black line of the STM image in Fig.  
40  
41 1(c), displays the typical height of these 3D clusters that is about 0.5 nm. In addition, it also exhibits  
42  
43 the height of the brighter area on the HOPG surface with respect to the darker region, which  
44  
45 amounts to  $0.25 \pm 0.05$  nm. Similar values are obtained measuring line profiles (e.g. see Fig. 1(e))  
46  
47 in other zones of the surface. Fig. 2 reports a blow-up around a few Si nanoclusters rising above  
48  
49 flatter areas. These flatter regions appear like a patchwork of hexagonal patterns with different  
50  
51 lattice spacing. Their extension, sometimes even larger than 6 nm (e.g. see Fig. 2a), prevents their  
52  
53 interpretation in terms of Moiré interferences or charge density waves induced on the HOPG  
54  
55 surface by the silicon deposition. [25,26] The white curve in Fig. 2(a) separates the area with lower  
56  
57  
58  
59  
60  
61  
62  
63  
64  
65

1  
2  
3  
4 lattice spacing (upper area) from the one with a larger lattice spacing (bottom part of the STM  
5 image). In Fig. 2(b), we report a 3D STM image, displaying the different height of the surface  
6 areas and the Si clusters. The bidimensional Fourier transform of the whole STM image reported  
7 in Fig. 2(a) shows two hexagonal spot patterns, one rotated by  $30^\circ$  with respect to the other (see  
8 Fig. 2(c)). The distance  $d$  between the spots and the center is  $\sqrt{3}/2 a$ , where  $a$  is the hexagonal  
9 lattice parameter. The first Fourier pattern (outer hexagonal spots) gives rise to a lattice spacing  
10 typical of HOPG ( $0.24 \pm 0.01$  nm). The inner hexagonal spots correspond to an  $a$  value of  $0.41 \pm$   
11  $0.02$  nm, which is a factor  $\sqrt{3}$  of the HOPG honeycomb lattice parameter. This is typical of a ( $\sqrt{3}$   
12  $\times \sqrt{3}$ ) $R30^\circ$  Si superstructure arranged on the carbon atom graphitic monolayer as reported in ref.  
13 [17] and [27]. In Fig. 2(d), we display a blow-up of the surface region with the largest lattice  
14 parameter. The honeycomb atomic arrangement on this surface is easily visible; a blue and red  
15 stick-and-ball model is superimposed on the STM experiment as guide to the eye. In ref. [17], we  
16 have already reported that the height difference of the atoms of the honeycomb lattice is  $0.05 \pm$   
17  $0.01$  nm. Our STM data support the results obtained by Persichetti *et al.* [28] and by L. Zhang *et*  
18 *al.* [29] indicating the formation of a few nanometer sized Germanene nanosheets around 3D Ge  
19 clusters on HOPG or MoS<sub>2</sub> surface defects, respectively. It is worth noting that in both cases the  
20 authors detected a lattice parameter of the atomic network typical of Germanene independently on  
21 the particular substrate. This is another piece of information suggesting that silicene is really  
22 formed around the 3D Si clusters and excluding any other HOPG surface artefacts. [25,26] On the  
23 other hand, our STM results are completely different from the ones reported by Chiappe *et al.* [18]  
24 and by van Bremen *et al.* [30] where Si has been deposited on a MoS<sub>2</sub> inert substrate and STM  
25 images showed no lattice parameter enlargement occurring on silicene formation. While the former  
26  
27  
28  
29  
30  
31  
32  
33  
34  
35  
36  
37  
38  
39  
40  
41  
42  
43  
44  
45  
46  
47  
48  
49  
50  
51  
52  
53  
54  
55  
56  
57  
58  
59  
60  
61  
62  
63  
64  
65

1  
2  
3  
4 interpreted these data in terms of a squeezing of the silicene lattice producing a huge buckling, the  
5  
6 latter suggested that a silicene layer intercalation occurred under the first atomic layer of MoS<sub>2</sub>.  
7  
8  
9

### 10 3.2 Raman analysis

11  
12  
13 Considering the insights about the coexistence of 3D silicon structures contiguous to silicene  
14 nanosheets obtained by STM analysis, we performed low magnification Raman line-scan maps  
15  
16 across the whole HOPG sample (Fig. S2 of ESM). We identify the three main Raman modes as  
17  
18 the graphite G and D bands as well as the bulk silicon TO mode peaked at 1580 cm<sup>-1</sup>, 1340 cm<sup>-1</sup>  
19 and 520 cm<sup>-1</sup>, respectively. We use the bulk silicon TO mode as the benchmark for promising areas  
20  
21 in which 3D silicon structures and silicene nanosheets coexist. Typical Raman spectra of bare  
22  
23 HOPG and silicon decorated HOPG surfaces, extrapolated from Fig. S2 are reported in Fig. S3 of  
24  
25 the ESM section.  
26  
27  
28  
29  
30  
31  
32  
33

34 Fig. 3(a) shows the typical Raman spectrum of three regions of the studied sample (green, red  
35 and black curves, for sake of clarity the spectra are shifted). The black curve corresponds to the  
36  
37 Raman features of a bare HOPG substrate, with its typical G and D bands. The intensity ratio  
38  
39 between D and G bands reveals an almost defect free HOPG, since the G band dominates over the  
40  
41 D band which is generally ascribed to defects. [16] This also means that upon Si deposition, not  
42  
43 all of the substrate surface is covered with silicon atoms. In the red and green curves, the Raman  
44  
45 spectrum is conversely dominated by features located around 520 cm<sup>-1</sup>. The HOPG Raman features  
46  
47 are still visible, but extremely reduced in intensity with respect to the dominant bulk Si resonance.  
48  
49 Notably, no Raman feature located around 800 cm<sup>-1</sup>, where silicon carbide modes are expected  
50  
51 [31], can be detected (see Fig. S4 in the ESM section). It is worth noting that, despite the absence  
52  
53  
54  
55  
56  
57  
58  
59  
60  
61  
62  
63  
64  
65

1  
2  
3  
4 of a capping layer, no sizeable Raman features due to silicon oxide are detectable in the spectra.  
5  
6 [32]

7  
8  
9  
10 Fig. 3(b) shows a blow-up around the Si 520  $\text{cm}^{-1}$  resonance. Both the red and green curves  
11 exhibit no evidence of amorphous silicon, which typically appears as a broad band centered at 480  
12  $\text{cm}^{-1}$ . [15] Both of these spectra can be fitted by using two Voigt curves, whose parameters are  
13  $\text{cm}^{-1}$ . [15] Both of these spectra can be fitted by using two Voigt curves, whose parameters are  
14  $\text{cm}^{-1}$ . [15] Both of these spectra can be fitted by using two Voigt curves, whose parameters are  
15 reported in Table S1 in ESM. The most intense Raman resonance peaks at 519.8  $\text{cm}^{-1}$  and has a  
16 very narrow FWHM (5  $\text{cm}^{-1}$ ), which is a typical for the bulk TO Si mode. [33] We ascribe this  
17 feature to large clusters. The peak located at 510  $\text{cm}^{-1}$ , with a FWHM as wide as 13.8  $\text{cm}^{-1}$ , could  
18 be assigned to Si nanoclusters with diameters smaller than the Bohr radius (5 nm), thus showing  
19 quantum confinement effects. [34] The attribution of these Raman modes to 3D Si clusters is  
20 corroborated by the presence of the weak, but wide feature extending between 900 and 1000  $\text{cm}^{-1}$ ,  
21 which is reported to correspond to two-phonon scattering (2TO) coming from Si in the  $\text{sp}^3$   
22 configuration (see Fig. S4 of SI). [35] The feature located at 542.5  $\text{cm}^{-1}$  has not been reported so  
23 far in the literature. Interestingly, its FWHM is as narrow as 7.2  $\text{cm}^{-1}$  and it is fully Gaussian. This  
24 suggests that we are dealing with a genuine crystalline vibrational mode that we interpret as the  
25 silicene mode.  
26  
27  
28  
29  
30  
31  
32  
33  
34  
35  
36  
37  
38  
39  
40  
41  
42  
43  
44

45 In order to go deeper in the Raman analysis and try to establish the nature of this new mode, we  
46 report in Fig. 4 the Raman maps obtained by collecting hundreds of Raman spectra over a 26  $\mu\text{m}$   
47 x 21  $\mu\text{m}$  region. Each pixel size is 500 nm x 500 nm. In the top-left panel of Fig. 4, the optical  
48 image of the surface is reported while the other panels, from Fig. 4(b) to Fig 4(f), display the maps  
49 of the peaks of the G and D bands of HOPG located at 1580  $\text{cm}^{-1}$  and 1340  $\text{cm}^{-1}$  and of the intensity  
50 of the peaks centered at 520  $\text{cm}^{-1}$ , 510  $\text{cm}^{-1}$ , 542.5  $\text{cm}^{-1}$  for the silicon structures, respectively.  
51  
52  
53  
54  
55  
56  
57  
58  
59  
60  
61  
62  
63  
64  
65

1  
2  
3  
4 Comparing these maps, we argue that the silicene Raman feature is quite diffused on the surface  
5  
6 although it is not present everywhere (see Fig. 4(f)). However, it is prevalently found in surface  
7  
8 areas close to large Si nano-clusters. Despite the giant difference in size between the areas probed  
9  
10 by Raman spectroscopy and by STM, there is a surprising similarity between the information given  
11  
12 by the two techniques. Moreover, thanks to this Raman mapping, we observe the silicene Raman  
13  
14 resonances in sample areas where the amplitude of the D band Raman features slightly increases  
15  
16 and no Si 3D cluster Raman features are detected. We interpret this result as the possibility of  
17  
18 silicene growth also occurring far away from 3D Si clusters.  
19  
20  
21  
22  
23

24  
25 From a theoretical point of view, stable free standing (FS) silicene has previously been reported  
26  
27 to present the Raman  $E_{2g}$  feature located at  $575\text{ cm}^{-1}$  [12] and a buckling value of 0.044 nm.  
28  
29 However, there are calculations where by varying the buckling of the FS silicene layer (without  
30  
31 addressing the energetic stability of the modified system), a downshift of the silicene  $E_{2g}$  feature  
32  
33 is observed with increasing buckling. [14] If one refers to Fig. 1 of the paper of Scalise *et al.*, [16]  
34  
35 the Raman  $E_{2g}$  peak for our STM experimental buckling of 0.05 nm is expected to occur around  
36  
37  $542.8\text{ cm}^{-1}$ . This Raman shift value fits very well with our experimental data (see Table S1 in SI  
38  
39 and Fig. 3(b)). Previous experimental Raman works showed an extreme reactivity of silicene  
40  
41 grown on Ag(111) surfaces to oxygen, which compelled the investigators to measure the Raman  
42  
43 spectra *in-situ* [14,15] or to cap the sample for *ex-situ* measurements. [11] This observation occurs  
44  
45 even in case of multilayer silicene samples. [36] Nevertheless, a Raman feature attributed to  
46  
47 silicene remains clearly visible while other studies reported that after air exposure the Raman peak  
48  
49 due to silicene disappears entirely after a short time. [11] We would like to underline the extreme  
50  
51 air-stability of our sample after having exposed it to air for several weeks allowing us to perform  
52  
53 the Raman measurements *ex-situ* without any capping. To understand this surprising air-stability  
54  
55  
56  
57  
58  
59  
60  
61  
62  
63  
64  
65

1  
2  
3  
4 deeper, we made a series of checks of the possible formation of silicon oxide. First of all, we  
5 performed Raman maps for several wavenumbers at which Si-O vibrational modes are expected,  
6  
7 i.e. around 430  $\text{cm}^{-1}$ , 600  $\text{cm}^{-1}$  and 1065  $\text{cm}^{-1}$ . [32] No relevant Raman amplitude can be detected  
8  
9 for maps set at frequencies equal to 600  $\text{cm}^{-1}$  and 1065  $\text{cm}^{-1}$ . Fig. 5a shows the Raman map  
10  
11 obtained at 430  $\text{cm}^{-1}$ , which corresponds to the highest strength mode among the silicon oxide  
12  
13 Raman features. Despite that the amplitude of this Raman mode is very low, one can observe a  
14  
15 small signal corresponding to sample areas mainly close to silicene detected far from Si 3D  
16  
17 nanoclusters. Furthermore, it looks as if the 3D Si clusters are not affected by the oxidation process.  
18  
19 To support these findings, we have performed X-ray photoemission spectroscopy measurements  
20  
21 on the 2p Si core level before and after air-exposure of the HOPG sample covered with 1 ML of  
22  
23 silicon. Fig. 5b shows a comparison between the two XPS spectra. Interestingly, we observed no  
24  
25 sizeable changes in the lineshape of 2p Si after air-exposure. It is worth noting that the presence  
26  
27 of silicon oxides is expected to produce a chemical shift up to 3.8 eV. [37] This means that, within  
28  
29 our XPS experimental resolution, no silicon oxide formation can be detected. Moreover, we  
30  
31 recorded the STM images (Fig. 5c) of the sample surface after air-exposure and we are still able  
32  
33 to observe the same morphology already shown in Fig. 2a, where a coexistence of 3D Si clusters  
34  
35 and atomically resolved silicene (brighter region) and HOPG networks (darker areas) are visible.  
36  
37 In Fig. 5d we exhibit a blow-up of the silicene region, indicated by the turquoise rectangular in  
38  
39 Fig. 5c, showing the atomic resolution of these nanosheets after air exposure. Note the good  
40  
41 coincidence with the stick and ball model of the silicene honeycomb lattice superimposed to the  
42  
43 experimental STM image.  
44  
45  
46  
47  
48  
49  
50  
51  
52  
53

54  
55  
56 We suggest that the very low reactivity with oxygen of silicene grown on HOPG compared to  
57  
58 that grown on Ag(111) can be related to the difference in the buckling value. Indeed, in the latter  
59  
60  
61  
62  
63  
64  
65

1  
2  
3  
4 case, the buckling has been estimated to vary between 0.07 and 0.1 nm, a value considerably higher  
5  
6 than the one measured in the present case (0.05 nm). This difference should give rise to a higher  
7  
8 contribution of  $sp^3$  components in the silicon honeycomb structure in the latter case, thus favoring  
9  
10 the presence of Si dangling bonds, which are highly reactive to oxygen. Our air stability results  
11  
12 are even better than those recently reported in ref. [38] on quasi-freestanding epitaxial silicene  
13  
14 grown on Ag(111) obtained by oxygen intercalation. The latter study has shown a gradual decrease  
15  
16 in intensity of the Raman  $E_{2g}$  feature with time and its complete disappearance after 6 days of air  
17  
18 exposure. Concerning the exceptional stability of the Si 3D nanoclusters upon air-exposure, it is  
19  
20 known that small Si nanoclusters are much less reactive to oxygen than the bulk because of the  
21  
22 high energy activation barrier that increases up to a factor of four with the decrease in Si cluster  
23  
24 size. [39] Moreover, in Fig. 6 we report the scanning tunneling spectroscopy (STS) for these small  
25  
26 Si nanoclusters before and after air-exposure. The  $V/I$   $dI/dV$  curves shown in Fig. 6 are  
27  
28 proportional to the filled and empty density of states close to the Fermi level ( $E_F$ ). [17] Due to non-  
29  
30 zero value assumed by both the curves close to the Fermi level, we conclude that these Si  
31  
32 nanoclusters are metallic in nature and remain metallic after air-exposure. The metal nature of very  
33  
34 small Si nanoclusters is theoretically expected when no H-saturation of the surface dangling bonds  
35  
36 is present. [7]

37  
38  
39  
40  
41  
42  
43  
44  
45  
46 To support our findings of silicene on HOPG, we have calculated theoretical spectra of these  
47  
48 structures. To validate the applied *ab initio* method, we have first calculated the spectrum of FS  
49  
50 silicene; the  $E_{2g}$  peak is found at  $556\text{ cm}^{-1}$  and lies in the range of published values from Refs.  
51  
52 [12,13]. The Si-Si bond length is 0.229 nm and the buckling is 0.049 nm. Two interfaces of silicene  
53  
54 and HOPG were studied, the rotation angles of the two hexagonal patterns were 10 and 30 degrees,  
55  
56 respectively. The modes which correspond to the  $E_{2g}$  mode are shown in Table 1. For both  
57  
58  
59  
60  
61  
62  
63  
64  
65

1  
2  
3  
4 interfaces a shortening of Si-Si bonds (0.226 nm and 0.227 nm for 10 and 30 degrees, respectively)  
5  
6 is observed in order to create a superlattice with HOPG. This also causes a slightly larger buckling  
7  
8 of 0.060 and 0.057 nm for 10 and 30 degrees, respectively. For 10 degrees, a blueshift of the  $E_{2g}$   
9  
10 modes to  $582\text{ cm}^{-1}$  is found; however for 30 degrees, we observe a redshift to  $540\text{-}544\text{ cm}^{-1}$ .  
11  
12 Experimentally, the pattern with a rotational angle of 30 degrees is dominant, thus we find an  
13  
14 excellent agreement between theory and experiment. One reason for the difference between the  
15  
16 interfaces are the structural parameters. Shortening of bond lengths leads to a blueshift, while  
17  
18 increased buckling leads to a redshift, where the former is more pronounced. For FS silicene, a  
19  
20 change of bond length from 0.227 to 0.226 nm (with constant buckling) blueshifts the frequency  
21  
22 by  $10\text{ cm}^{-1}$ , while changing the buckling from 0.057 to 0.060 nm redshifts it only by  $1\text{ cm}^{-1}$ . The  
23  
24 difference of shifts for 10 and 30 degrees indicates that the Raman frequencies are very sensitive  
25  
26 to strain in silicene caused by pattern creation with the HOPG substrate. However, the  
27  
28 experimentally observed silicene nanosheets have a finite size whereas all previous calculations  
29  
30 consider infinite systems only. In order to evaluate the influence of strain for finite size silicene,  
31  
32 we calculated the spectra of four nano-islands of silicene (see Fig. 7) with side lengths of 1.3-1.5  
33  
34 nm and similar shape as in Fig 2(d), which differ in the edge type (zigzag and armchair) and  
35  
36 rotation angle (10 and 30 degrees). The average bond length increases to 0.228 nm (for all nano-  
37  
38 islands) due to the removal of periodic constraints with respect to the interfaces; buckling is  
39  
40 reduced to 0.052-0.053 nm after optimization. We obtain a redshift for all nano-islands to about  
41  
42  $542\text{-}550\text{ cm}^{-1}$  (see Fig. S6 in ESM for pictures of the modes). These theoretical results agree very  
43  
44 well with both our experiments and our values calculated for the infinite silicene layer at 30  
45  
46 degrees. We like, therefore, to conclude that the IF-30 is likely to experience a similar amount of  
47  
48 strain as the nano islands which resemble the real experimentally observed system more closely.  
49  
50  
51  
52  
53  
54  
55  
56  
57  
58  
59  
60  
61  
62  
63  
64  
65

1  
2  
3  
4 4. Conclusions  
5  
6  
7

8 In conclusion, though the growth mechanism of Si on the HOPG surface is prevalently three-  
9 dimensional, our present study confirms that silicene nanosheets can be observed upon silicon  
10 deposition at room temperature on such an inert substrate. Raman spectra show, in fact, the  
11 appearance of a new feature located at  $542.5\text{ cm}^{-1}$  never reported so far in the literature. The present  
12 Raman peak of silicene is located markedly far in wavenumbers from those reported for the several  
13 phases of silicene grown on Ag(111) surfaces. Moreover, this Raman resonance value is different  
14 from all previously observed ones for all known Si configurations, including amorphous silicon,  
15 3D clusters of every size, and bulk Si in  $sp^3$  configurations. Based on our *ab initio* calculations,  
16 we attribute the measured Raman shift to the strain that the finite size silicene nanosheets  
17 experience due to the interaction with the graphite substrate. Most importantly, we have shown for  
18 our small nano sheets that silicene grown on an inert substrate like HOPG is remarkably stable in  
19 air for at least several weeks, which we attribute to the observed low buckling and the resulting  
20 small number of dangling bonds.  
21  
22  
23  
24  
25  
26  
27  
28  
29  
30  
31  
32  
33  
34  
35  
36  
37  
38  
39

40 Electronic Supplementary Material: Supplementary material is available in the online version of  
41 this article at [http://dx.doi.org/10.1007/\\*\\*\\*\\*\\*](http://dx.doi.org/10.1007/*****)  
42  
43  
44  
45

46 References  
47

48 [1] Novoselov, K. S.; Geim, A. K.; Morozov, S. V. ; Jiang, D.; Zhang, Y.; Dubonos, S. V. ;  
49 Grigorieva, I. V.; Firsov, A. A. Electric field effect in atomically thin carbon films. *Science*  
50 **2004**, *306*, 666–669.  
51  
52  
53  
54  
55  
56  
57  
58  
59  
60  
61  
62  
63  
64  
65

- 1  
2  
3  
4 [2] Novoselov, K. S.; Geim, A. K.; Morozov, S. V.; Jiang, D. ; Katsnelson, M. I. ; Grigorieva,  
5  
6 I. V. ; Dubonos, S. V. ; Firsov, A. A. Two-Dimensional Gas of Massless Dirac Fermions  
7  
8 in Graphene. *Nature* **2005**, *438*, 197-200.  
9  
10  
11  
12 [3] Novoselov, K. S.; Jiang, Z. ; Zhang, Y. ; Morozov, S. V.; Stormer, H. L.; Zeitler, U.;  
13  
14 Maan, J. C.; Boebinger, G. S.; Kim, P.; Geim, A. K. Room-temperature quantum Hall  
15  
16 effect in graphene. *Science* **2007**, *315*, 1379-1379.  
17  
18  
19  
20  
21 [4] Lee, C.; Wei, X.; Kysar, J. W.; Hone, J. Measurement of the Elastic Properties and Intrinsic  
22  
23 Strength. *Science* **2008**, *321*, 385-388.  
24  
25  
26  
27 [5] Geim, A. K.; Novoselov, K. S. The Rise of Graphene. *Nat. Mater.* **2007**, *6*, 183-191.  
28  
29  
30  
31 [6] Scheier, P.; Marsen, B.; Lonfat, M.; Schneider, W.-D.; Sattler, K. Growth of silicon  
32  
33 nanostructures on graphite. *Surf. Sci.* **2000**, *458*, 113–122.  
34  
35  
36  
37 [7] Mélinon, P.; Kéghélian, P.; Prével, B.; Perez, A.; Guiraud, G.; LeBrusq, J.; Lermé, J.;  
38  
39 Pellarin, M.; Broyer, M. Nanostructured silicon films obtained by neutral cluster  
40  
41 depositions. *J. Chem. Phys.* **1997**, *107*, 10278-10287.  
42  
43  
44  
45 [8] Katircioglu, Ş.; Erkoç, Ş. Structural and electronic properties of bare and hydrogenated  
46  
47 silicon clusters. *Physica E* **2001**, *9*, 314-320.  
48  
49  
50  
51 [9] Cahangirov, S.; Topsakal, M.; Akturk, E.; Sahin, H.; Ciraci, S. Two- and one-dimensional  
52  
53 honeycomb structures of silicon and germanium. *Phys. Rev. Lett.* **2009**, *102*, 236804.  
54  
55  
56  
57  
58  
59  
60  
61  
62  
63  
64  
65

- 1  
2  
3  
4 [10] Vogt, P.; De Padova, P.; Quaresima, C.; Avila, J.; Frantzeskakis, E.; Asensio, M.  
5  
6 C.; Resta, A.; Ealet, B.; Le Lay, G. Silicene: Compelling Experimental Evidence for  
7  
8 Graphenelike Two-Dimensional Silicon. *Phys. Rev. Lett.* **2012**, *108*, 155501.  
9  
10  
11  
12 [11] Tao, L.; Cinquanta, E.; Chiappe, D.; Grazianetti, C.; Fanciulli, M.; Dubey, M.;  
13  
14 Molle, A.; Akinwande, D. Silicene field-effect transistors operating at room temperature.  
15  
16  
17 *Nat. Nanotechnol.* **2015**, *10*, 227–231.  
18  
19  
20  
21 [12] Scalise, E.; Houssa, M.; Pourtois, G.; van den Broek, B.; Afanas'ev, V.; Stesmans  
22  
23 A. Vibrational properties of silicene and germanene. *Nano Research* **2013**, *6*, 19–28.  
24  
25  
26  
27 [13] Yan, J.-A.; Stein, R.; Schaefer, D. M.; Wang, X.-Q.; Chou, M. Y. Electron-phonon  
28  
29 coupling in two-dimensional silicene and germanene. *Phys. Rev. B* **2013**, *88*, 121403(R).  
30  
31  
32  
33 [14] Zhuang, J.; Xu, X.; Du, Y.; Wu, K.; Chen, L.; Hao, W.; Wang, J.; Yeoh, W. K.;  
34  
35 Wang, X.; Dou, S. X. Investigation of electron-phonon coupling in epitaxial silicene by in  
36  
37 situ Raman spectroscopy. *Phys. Rev. B* **2015**, *91*, 161409(R).  
38  
39  
40  
41 [15] Solonenko, D.; Gordan, O. D.; Le Lay, G.; Sahin, H.; Cahangirov, S.; Zahn, D.  
42  
43 R. T.; Vogt, P. 2D vibrational properties of epitaxial silicene on Ag(111). *2D Mater.*  
44  
45 **2016**, *4*, 015008.  
46  
47  
48  
49 [16] Scalise, E.; Cinquanta, E.; Houssa, M.; van den Broek, B.; Chiappe, D.;  
50  
51 Grazianetti, C.; Pourtois, G.; Ealet, B.; Molle, A. Fanciulli M, Afanas'ev V V, Stesmans  
52  
53 A. Vibrational properties of epitaxial silicene layers on (111) Ag. *Appl. Surf. Sci.* **2014**,  
54  
55 *291*, 113– 117.  
56  
57  
58  
59  
60  
61  
62  
63  
64  
65

- 1  
2  
3  
4 [17] De Crescenzi, M.; Berbezier, I.; Scarselli, M.; Castrucci, P. ; Abbarchi, M. ; Ronda,  
5  
6 A. ; Jardali, F.; Park, J. ; Vach, H. Formation of Silicene Nanosheets on Graphite. *ACS*  
7  
8 *Nano* **2016**, *10*, 11163–11171.  
9  
10  
11  
12 [18] Chiappe, D.; Scalise, E.; Cinquanta, E.; Grazianetti, C.; van den Broek, B.;  
13  
14 Fanciulli, M.; Houssa, M.; Molle, A. Two-Dimensional Si Nanosheets with Local  
15  
16 Hexagonal Structure on a MoS<sub>2</sub> Surface. *Adv. Materials* **2014**, *26*, 2096-2101.  
17  
18  
19  
20 [19] Dovesi, R. ; Civalleri, B. ; Roetti, C. ; Saunders, V. R. ; Zicovich-Wilson, C. M.  
21  
22 CRYSTAL: A computational tool for ab initio study of the electronic properties of crystals.  
23  
24 *Z. Kristallogr.* **2005**, *220*, 571-573.  
25  
26  
27  
28 [20] Dovesi, R.; Saunders, V. R.; Roetti, C.; Orlando, R.; Zicovich-Wilson, C. M.;  
29  
30 Pascale, F.; , Civalleri, B.; Doll, K.; Harrison, N. M.; Bush, J. J.; D'Arco, Ph.; Llunell, M.  
31  
32 CRYSTAL09 User's Manual (University of Torino, Torino, 2009).  
33  
34  
35  
36  
37 [21] Perdew, J. P.; Burke, K.; Ernzerhof, M. Generalized Gradient Approximation  
38  
39 Made Simple. *Phys. Rev. Lett.* **1996**, *77*, 3865-3868.  
40  
41  
42  
43 [22] Grimme, S. Semiempirical GGA-Type Density Functional Constructed with a  
44  
45 Long-Range Dispersion Correction. *J. Comput. Chem.* **2006**, *27*, 1787-1799.  
46  
47  
48  
49 [23] Pascale, F.; Zicovich-Wilson, C. M.; Lopez, F.; Civalleri, B.; Orlando, R.; Dovesi  
50  
51 R. The Calculation of the Vibration Frequencies of Crystalline Compounds and Its  
52  
53 Implementation in the CRYSTAL Code. *J. Comput. Chem.* **2004**, *25*, 888-897.  
54  
55  
56  
57  
58  
59  
60  
61  
62  
63  
64  
65

- 1  
2  
3  
4 [24] Zicovich-Wilson, C. M.; Pascale, F.; Roetti, C.; Saunders, V. R.; Orlando, R.;  
5  
6 Dovesi, R. The Calculation of the Vibration Frequencies of alpha-Quartz: The Effect of  
7  
8 Hamiltonian and Basis Set. *J. Comput. Chem.* **2004**, *25*, 1873-1881.  
9  
10  
11  
12 [25] Ferro, Y.; Thomas, C.; Angot, T.; Génésio, T.; Allouche, A. Theoretical and  
13  
14 experimental characterization of damaged graphite surfaces. *Journal of Nuclear Materials*  
15  
16 **2007**, *363–365*, 1206–1210.  
17  
18  
19  
20 [26] Büttner, M.; Choudhury, P.; Johnson, J. K.; Yates, J. T. Jr. Vacancy clusters as  
21  
22 entry ports for cesium intercalation in graphite. *Carbon* **2011**, *49*, 3937-3952.  
23  
24  
25  
26 [27] Cai, Y.; Chuu, C.-P.; Wei, C. M.; Chou, M. Y. Stability and electronic properties  
27  
28 of two-dimensional silicene and germanene on graphene. *Phys. Rev. B* **2013**, *88*, 245408  
29  
30 (2013).  
31  
32  
33  
34 [28] Persichetti, L.; Jardali, F.; Vach, H.; Sgarlata, A.; Berbezier, I.; De Crescenzi, M.;  
35  
36 & Balzarotti, A. van der Waals Heteroepitaxy of Germanene Islands on Graphite. *J. Phys.*  
37  
38 *Chem. Lett.* **2016**, *7*, 3246–3251.  
39  
40  
41  
42 [29] Zhang, L.; Bampoulis, P.; Rudenko, A. N.; Yao, Q.; van Houselt, A.; Poelsema, B.;  
43  
44 Katsnelson, M. I. & Zandvliet, H. J. W. Structural and Electronic Properties of Germanene  
45  
46 on MoS<sub>2</sub>. *Phys. Rev. Lett.* **2016**, *116*, 256804.  
47  
48  
49  
50  
51 [30] van Bremen, R.; Yao, Q.; Banerjee, S.; Cakir, D.; Oncel, N.; & Zandvliet, H. J. W.  
52  
53 Intercalation of Si between MoS<sub>2</sub> layers. *Beilstein J. Nanotechnol.* **2017**, *8*, 1952–1960.  
54  
55  
56  
57  
58  
59  
60  
61  
62  
63  
64  
65

- 1  
2  
3  
4 [31] Nakashima, S.; Harima, H. Raman Investigation of SiC Polytypes. *Phys. Stat. Sol.*  
5  
6 (a) **1997**, *162*, 39-64.  
7  
8  
9  
10 [32] Borowicz, P.; Latek, M.; Rzodkiewicz, W.; Łaszcz, A.; Czerwinski, A.; Ratajczak,  
11  
12 J. Deep-ultraviolet Raman investigation of silicon oxide. *Adv. Nat. Sci.: Nanosci.*  
13  
14 *Nanotechnol.* **2012**, *2*, 045003.  
15  
16  
17  
18 [33] Parker, J. H.; Feldman, D. W.; Ashkin, M. Raman Scattering by Silicon and  
19  
20 Germanium. *Physical Review* **1967**, *155*, 712-714.  
21  
22  
23  
24 [34] Faraci, G.; Gibilisco, S.; Pennisi, A. R. Quantum confinement and thermal effects  
25  
26 on the Raman spectra of Si nanocrystals. *Phys. Rev. B* **2009**, *80*, 193410.  
27  
28  
29  
30 [35] Temple, P. A.; Hathaway, C. E. Multiphonon Raman Spectrum of Silicon. *Phys.*  
31  
32 *Rev. B* **1973**, *7*, 3685.  
33  
34  
35  
36 [36] De Padova, P.; Ottaviani, C.; Quaresima, C.; Olivieri, B.; Imperatori, P.; Salomon,  
37  
38 E.; Angot, T.; Quaglian, L.; Romano, C.; Vona, A.; Muniz-Miranda, M.; Generosi, A.;  
39  
40 Paci, B.; Le Lay, G. 24 h stability of thick multilayer silicene in air. *2D Materials* **2014**,  
41  
42 *1*, 021003.  
43  
44  
45  
46 [37] Himpsel, F. J.; McFeely, F. R.; Taleb-Ibrahimi, A.; Yarmoff, J. A.; Hollinger, G.  
47  
48 Microscopic structure of the SiO<sub>2</sub>/Si interface. *Phys. Rev. B* **1988**, *38*, 6084.  
49  
50  
51  
52 [38] Du, Y.; Zhuang, J.; Wang, J.; Li, Z.; Liu, H.; Zhao, J.; Xu, X.; Feng, H.; Chen, L.;  
53  
54 Wu, K.; Wang, X.; Dou, S. X. Quasi-freestanding epitaxial silicene on Ag (111) by oxygen  
55  
56 intercalation. *Sci. Adv.* **2016**, *2*, e1600067.  
57  
58  
59  
60  
61  
62  
63  
64  
65

1  
2  
3  
4  
5  
6  
7  
8  
9  
10  
11  
12  
13  
14  
15  
16  
17  
18  
19  
20  
21  
22  
23  
24  
25  
26  
27  
28  
29  
30  
31  
32  
33  
34  
35  
36  
37  
38  
39  
40  
41  
42  
43  
44  
45  
46  
47  
48  
49  
50  
51  
52  
53  
54  
55  
56  
57  
58  
59  
60  
61  
62  
63  
64  
65

[39] Jarrold, M. F.; Ray, U.; Creegan, K. M. Chemistry of semiconductor clusters: Large silicon clusters are much less reactive towards oxygen than the bulk. *J. Chem. Phys.* **1990**, *93*, 224.

### Acknowledgments

H.V., F.J., and C.L. gratefully acknowledge the HPC centers of the EDF, IDRIS (Grant i2016-090642), and CERMM for computational resources and the Hariri Foundation for Sustainable Human Development for the scholarship awarded to F.J.. M.D.C., P.C., M.S. and M.S. would like to acknowledge the European Community for the RISE Project CoExAN GA644076 and the project “Silicene and Germanene: novel two-dimensional nanomaterial” funded by the University of Roma Tor Vergata (Italy).

Table 1 Theoretical Raman shifts for several silicene configurations

Theoretical frequencies in  $\text{cm}^{-1}$  for the two Raman-active modes for free-standing silicene (Silicene), the infinite interfaces at 10 (IF-10) and 30 (IF-30) degrees rotational angle, the armchair edge nano-islands with 10 (NI-AC-10) and 30 (NI-AC-30) degrees rotational angle and zigzag nano-islands with 10 (NI-ZZ-10) and 30 (NI-ZZ-30) degrees rotational angle.

	<b>Mode 1 (<math>\text{cm}^{-1}</math>)</b>	<b>Mode 2 (<math>\text{cm}^{-1}</math>)</b>
Silicene	555.6	
IF-10	584.1	582.9
IF-30	539.8	546.3
NI-AC-10	542.4	550.8
NI-AC-30	550.5	542.1
NI-ZZ-10	546.5	546.2
NI-ZZ-30	545.9	545.5

1  
2  
3  
4 Figure Captions  
5  
6  
7  
8

9 Figure 1. (a) Low magnification STM image ( $V_{\text{sample}}=+0.3$  V,  $I_{\text{tunn}}=0.3$  nA) after one silicon  
10 monolayer deposited on a HOPG substrate at RT, showing the decoration of the atomic  
11 steps of HOPG by silicon clusters. Larger magnification STM image (b) and (c)  
12 magnification of the yellow area highlighted in (b). (d) and (e) Height line profile along  
13 the black and blue arrows shown in (c), respectively. The areas which appear brighter  
14 with respect to the substrate are related to silicene nanosheets. The average height of  
15 flat silicon clusters is less than 1 nm.  
16  
17  
18  
19  
20  
21  
22  
23  
24  
25  
26  
27

28  
29 Figure 2 (a) STM images ( $V_{\text{sample}}=+0.3$  V,  $I_{\text{tunn}}=0.3$  nA) after one silicon monolayer deposited  
30 on a HOPG substrate at RT. Note the coexistence of a silicene nanosheet and some  
31 silicon nano clusters (white regions) with a height of less than 1 nm. (b) Three  
32 dimensional reconstruction of image (a); (c) Bi-dimensional Fourier Transform of the  
33 STM image in panel (a): two hexagons (the external one due to HOPG and the internal  
34 one to silicene) rotated by about  $30^\circ$  one with respect to the other. (d) Blow up of a  
35 particular area from (a) with the superimposition of the stick-and-ball model showing  
36 the honeycomb structure of silicene, blue and red atoms are slightly buckled by about  
37 0.05 nm (the line profile displaying the height of the buckling has been already  
38 reported in ref. 17).  
39  
40  
41  
42  
43  
44  
45  
46  
47  
48  
49  
50  
51  
52  
53

54  
55 Figure 3 (a) Raman spectroscopy of promising areas of the HOPG sample after the deposition  
56 of 1 ML of silicon: the black line shows the standard Raman modes of bare graphite,  
57 the red line shows a peculiar Raman mode at  $510\text{ cm}^{-1}$  due to quantum confined silicon  
58  
59  
60  
61  
62  
63  
64  
65

1  
2  
3  
4 nanocrystals (size less than 5 nm) and at  $520\text{ cm}^{-1}$  due to Si TO, and the green line  
5 shows the Raman resonance at  $520\text{ cm}^{-1}$  due to the TO Si mode; (b) A blow-up around  
6  
7  
8  
9  
10  
11  
12  
13  
14  
15  
16  
17  
18  
19  
20  
21  
22  
23  
24  
25  
26  
27  
28  
29  
30  
31  
32  
33  
34  
35  
36  
37  
38  
39  
40  
41  
42  
43  
44  
45  
46  
47  
48  
49  
50  
51  
52  
53  
54  
55  
56  
57  
58  
59  
60  
61  
62  
63  
64  
65

Figure 4 (a) High magnification confocal optical image (100X objective), (b) the G band intensity map, (c) the D Band intensity map, (d) the Si TO mode, (e) the mode of quantum confined silicon nano-clusters, and (f) the  $E_{2g}$  mode of low-buckled silicene. Note that the silicene mode (yellow spots) is present in many areas of the surface, often but not always close to 3D Si nanoclusters.

Figure 5 (a) High magnification Raman mode located at  $430\text{ cm}^{-1}$ , frequency generally ascribed to silicon oxides. This Raman map has been obtained in the same surface region already reported in Fig. 4. Compare the position of silicon oxides with the modes due to SiNCs, silicene and carbon D and G band (b) XPS Si 2p level spectra before and after air-exposure. No differences between the two spectra are detected within the experimental resolution. In particular, no feature due to silicon oxide and suboxides is observed. The two curves have been arbitrarily normalized and shifted for clarity. (c) STM image of the sample after air-exposure. Note the presence of 3D Si nanoclusters (brightest spots whose height is very similar to that reported in Fig. 1), silicene nanosheets (brighter regions) and graphite substrate (darker areas). The difference in height between these two regions is less than 1 nm, as obtained before exposure to air. (d) Blow-up of the brighter region indicated by the turquoise rectangular, showing the atomic resolution in the silicene nanosheet after air exposure. Note the good

1  
2  
3  
4 coincidence with the stick and ball model of the silicene honeycomb lattice  
5  
6 superimposed to the experimental STM image.  
7  
8  
9

10 Figure 6 (a)  $V/I$   $dI/dV$  of the current-voltage (I-V) curves recorded on Si nanoclusters before  
11 (black curve) (see Fig. 1b and 1c) and after (see Fig. 5c) air-exposure (red curve). The  
12  $V/I$   $dI/dV$  curves are proportional to the electronic density of states. Note the metallic  
13 character of both the curves, due to the finite value of the density of states close to the  
14 Fermi level.  
15  
16  
17  
18  
19  
20  
21  
22

23 Figure 7 Optimized structures of armchair edge nano-islands with (a) 10 degrees and (b) 30  
24 degrees rotational angle and zigzag nano-islands with (c) 10 degrees and (d) 30 degrees  
25 rotational angle; hydrogen atoms are omitted for better visibility, higher and lower Si  
26 atoms due to buckling are shown in red and blue, respectively.  
27  
28  
29  
30  
31  
32  
33  
34  
35  
36  
37  
38  
39  
40  
41  
42  
43  
44  
45  
46  
47  
48  
49  
50  
51  
52  
53  
54  
55  
56  
57  
58  
59  
60  
61  
62  
63  
64  
65

Fig. 1

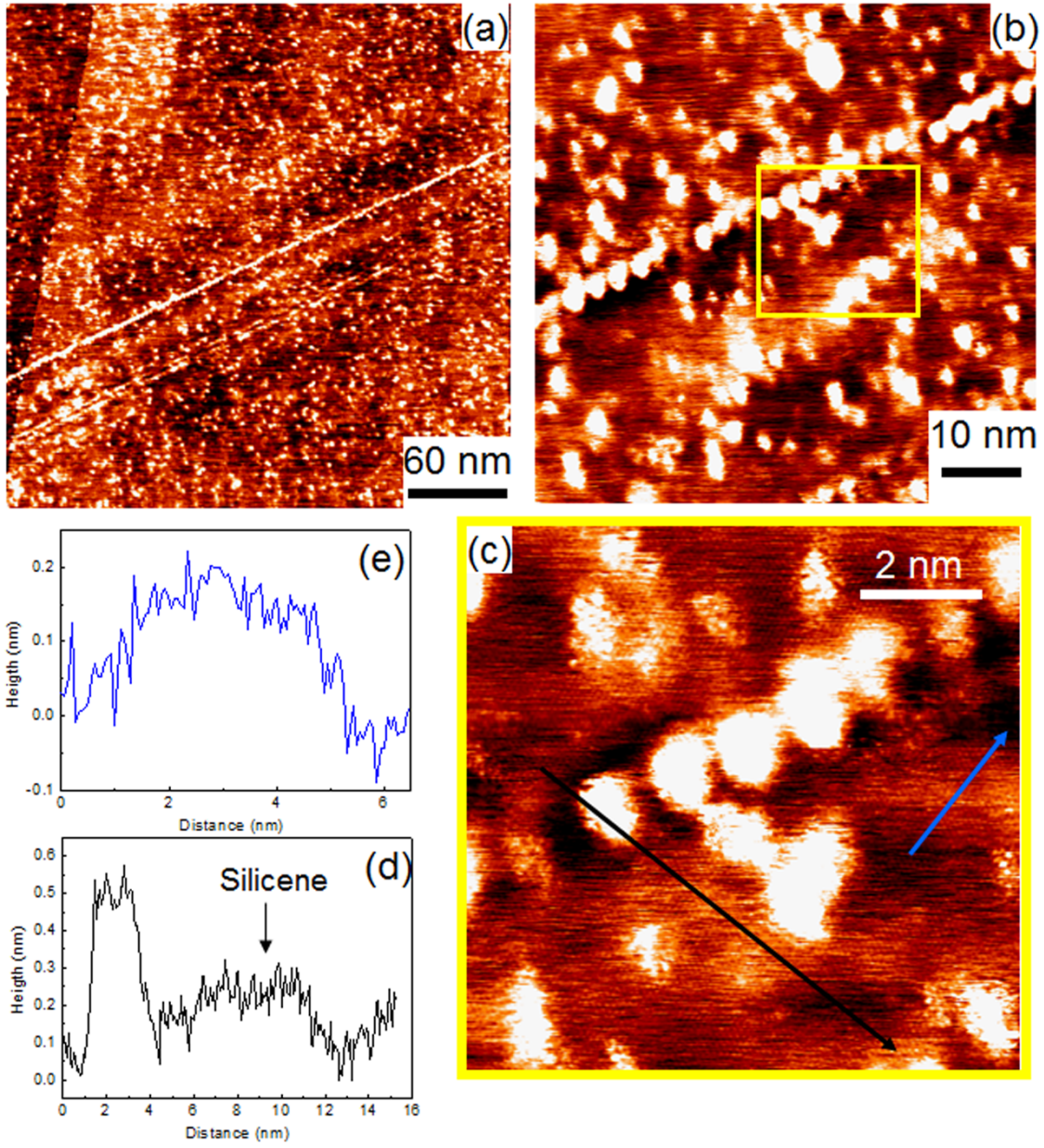


Fig. 2

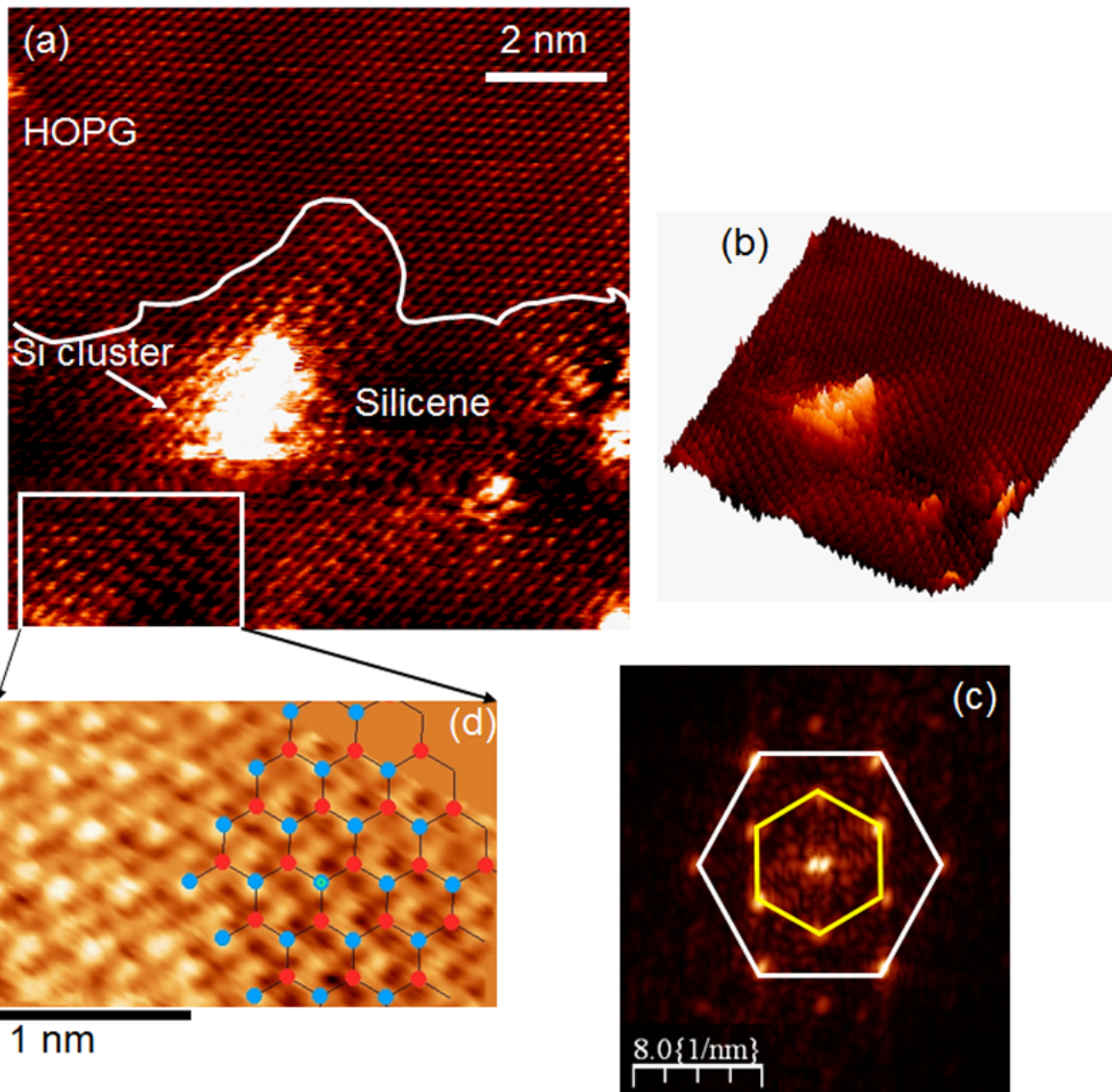


Fig. 3

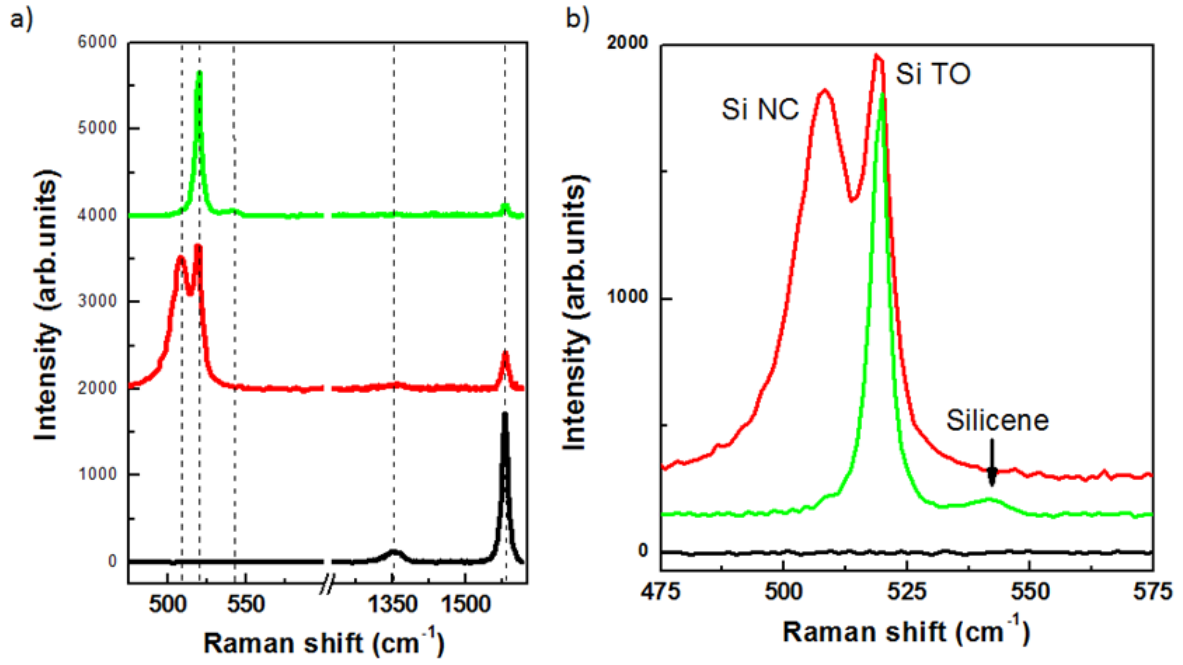


Fig. 4

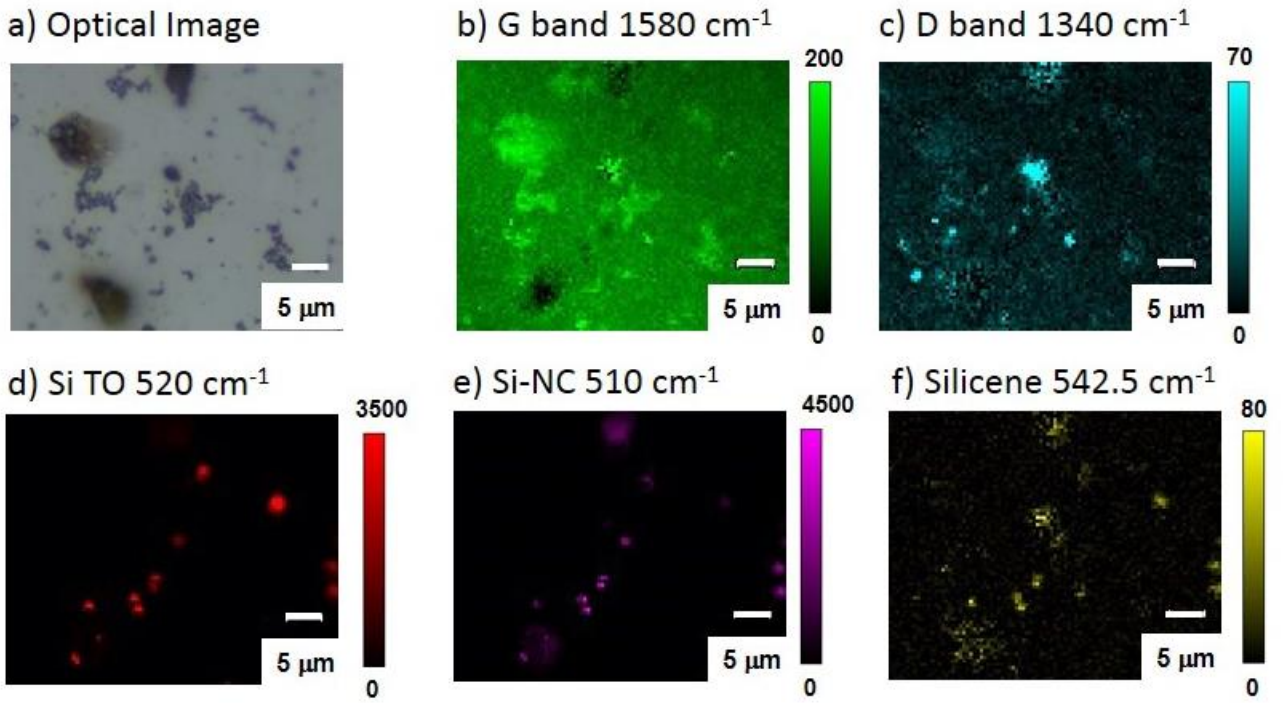
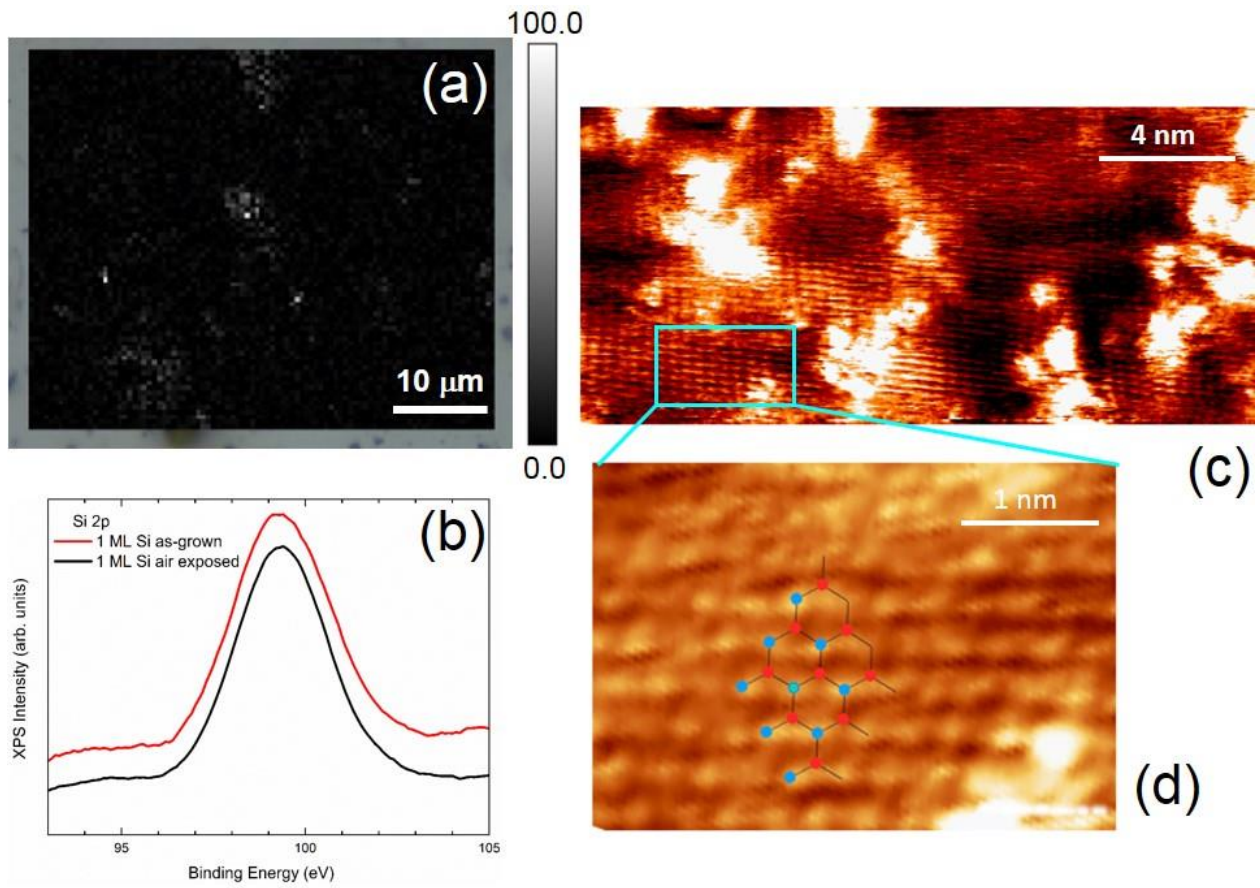
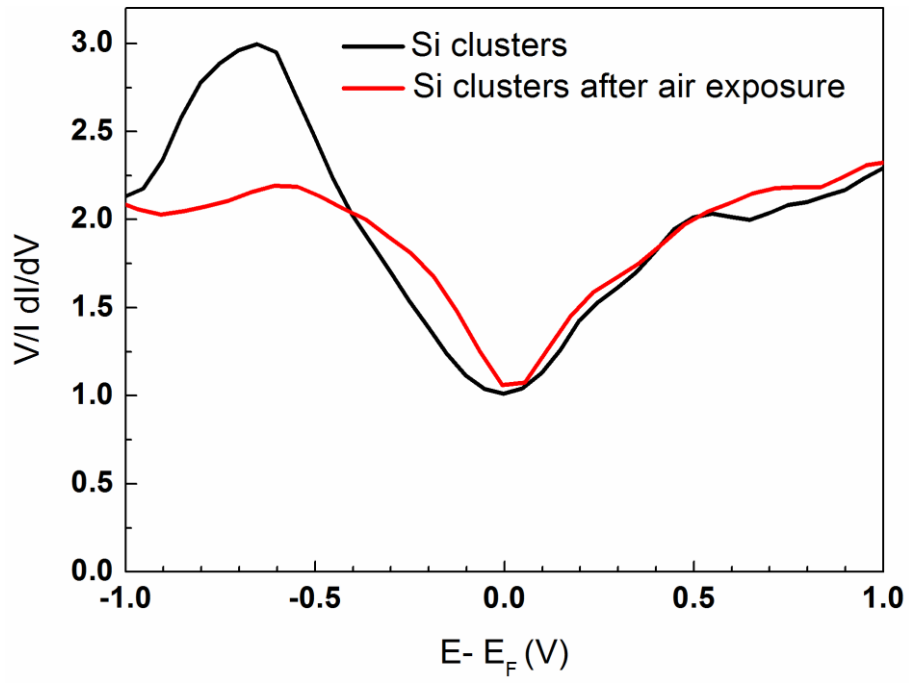


Fig. 5



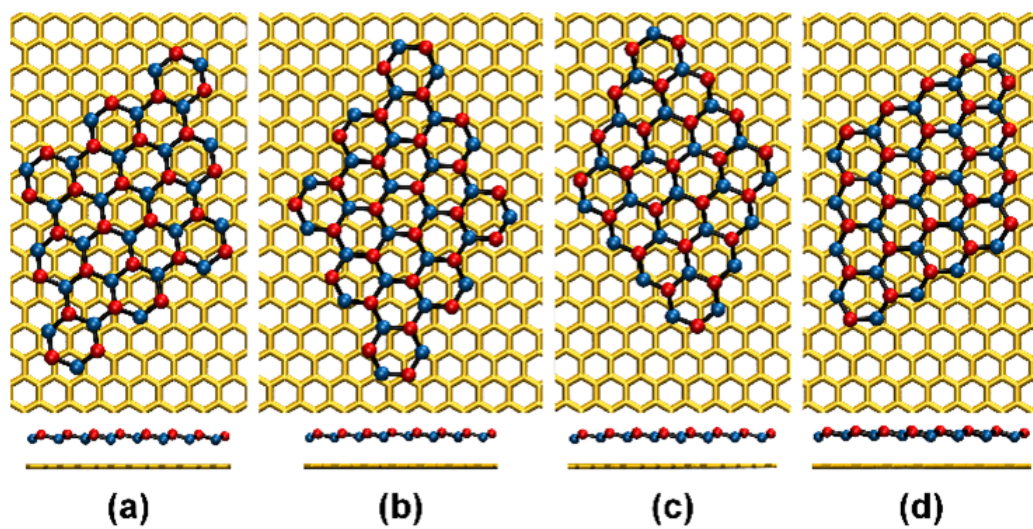
1  
2  
3  
4  
5  
6  
7  
8  
9  
10  
11  
12  
13  
14  
15  
16  
17  
18  
19  
20  
21  
22  
23  
24  
25  
26  
27  
28  
29  
30  
31  
32  
33  
34  
35  
36  
37  
38  
39  
40  
41  
42  
43  
44  
45  
46  
47  
48  
49  
50  
51  
52  
53  
54  
55  
56  
57  
58  
59  
60  
61  
62  
63  
64  
65

Fig. 6



1  
2  
3  
4  
5  
6  
7  
8  
9  
10  
11  
12  
13  
14  
15  
16  
17  
18  
19  
20  
21  
22  
23  
24  
25  
26  
27  
28  
29  
30  
31  
32  
33  
34  
35  
36  
37  
38  
39  
40  
41  
42  
43  
44  
45  
46  
47  
48  
49  
50  
51  
52  
53  
54  
55  
56  
57  
58  
59  
60  
61  
62  
63  
64  
65

Fig. 7





Click here to access/download  
**Supplementary Material**  
Electronic Supplementary Materials.docx

